

## Effect of laser polarization on QED cascading

V. F. Bashmakov,<sup>1,2</sup> E. N. Nerush,<sup>1,2</sup> I. Yu. Kostyukov,<sup>1,2, a)</sup> A. M. Fedotov,<sup>3</sup> and N. B. Narozhny,<sup>3</sup>

<sup>1)</sup>*Institute of Applied Physics, Russian Academy of Sciences, 603950 Nizhny Novgorod, Russia*

<sup>2)</sup>*University of Nizhny Novgorod, 23 Gagarin Avenue, Nizhny Novgorod 603950, Russia*

<sup>3)</sup>*National Research Nuclear University MEPhI, Moscow, 115409, Russia*

Development of QED cascades in a standing electromagnetic wave for circular and linear polarizations is simulated numerically with a 3D PIC-MC code. It is demonstrated that for the same laser energy the number of particles produced in a circularly polarized field is greater than in a linearly polarized field, though the acquiring mean energy per particle is larger in the latter case. The qualitative model of laser-assisted QED cascades is extended by including the effect of polarization of the field. It turns out that cascade dynamics is notably more complicated in the case of linearly polarized field, where separation into the qualitatively different "electric" and "magnetic" regions (where the electric field is stronger than the magnetic field and vice versa) becomes essential. In the "electric" regions acceleration is suppressed and moreover the high-energy electrons are even getting cooled by photon emission. The volumes of the "electric" and "magnetic" regions evolve periodically in time, and so does the cascade growth rate. In contrast to the linear polarization the charged particles can be accelerated by circularly polarized wave even in "magnetic region". The "electric" and "magnetic" regions do not evolve in time and cascade growth rate almost does not depend on time for circular polarization.

PACS numbers: 12.20.-m, 42.50.Ct, 52.27.Ep, 52.25.Dg

Keywords: electromagnetic cascades, strong laser field, kinetic equations, Monte Carlo simulations

---

<sup>a)</sup>Electronic mail: kost@appl.sci-nnov.ru

## I. INTRODUCTION

Quantum electrodynamical (or electromagnetic) cascades play an important role in astrophysical phenomena. Cascades initiated by high energy cosmic rays produce electromagnetic showers in magnetospheres and atmospheres of planets<sup>1</sup>. It is generally believed that cascading is a key mechanism of electron-positron plasma production at the neutron stars<sup>2</sup>. Recently QED cascading in strong laser field has attracted significant attention<sup>3-5</sup>. Interest to laser-assisted QED cascading comes due to a rapid progress in laser technology which opens opportunities to study the high-field QED effects under the laboratory conditions with the upcoming high-power laser facilities<sup>6,7</sup>.

A cascade develops as a sequence of elementary QED processes: photon emission by relativistic charged particles in the field of a nucleus or in an external electromagnetic field alternates with photon decay by a pair production. Such an order of the events leads to an avalanche-like production of electron-positron plasma and  $\gamma$ -quanta. In the case of electromagnetic showers the energy of the cascade particles is retrieved exclusively from the energy of the incoming cosmic ray. However, the cascade energy can also be gained from the external electromagnetic field as, e.g. in the vicinity of a surface of a pulsar or in laser-assisted QED cascades. In the latter case the electrons and the positrons produced during cascade development are accelerated in the laser field.

Laser acceleration is capable for boosting up the energy of the charged particles and, more notably, for turning them around transversely to the field, thus increasing dramatically the probabilities of QED processes and, accordingly, the cascading rate. If the plasma resulting from cascading becomes rather dense, the self-generated plasma field can become even as strong as the laser field itself. In such a case the laser field can be significantly depleted because of the avalanche-like electron-positron plasma production and  $\gamma$ -ray emission<sup>5</sup>. In this way QED cascades may limit the attainable intensity of the focused laser pulses<sup>4</sup>.

The QED cascade can be seeded either by external particles injected in the laser focal spot, or even by the pairs created due to vacuum breakdown. Electron-positron plasma can be produced also directly via vacuum breakdown in the strong electromagnetic field, but in order to produce dense enough electron-positron plasma by this way the field strength has to be of the order of the QED critical field,  $E_{cr} = m^2 c^3 / e \hbar \simeq 1.3 \times 10^{16}$  V/cm<sup>8-10</sup>, where  $e > 0$  and  $m$  are the value of electron charge and the electron mass, respectively. However, the

cascades in the presence of a seed appear already at much lower values of the field strength.

One of the key QED parameters that determine the probability of photon emission and radiation regime is and radiation regime is<sup>11,12</sup>

$$\chi = \frac{e\hbar}{m^3c^4} \sqrt{\left(\frac{\varepsilon\mathbf{E}}{c} + \mathbf{p} \times \mathbf{B}\right)^2 - (\mathbf{p} \cdot \mathbf{E})^2}, \quad (1)$$

where  $\mathbf{E}$  and  $\mathbf{B}$  are the electric and the magnetic fields,  $\varepsilon$  and  $\mathbf{p}$  are the energy and the momentum of an electron (positron). As was discussed in<sup>4,9,10</sup>, below the QED critical field and for optical range it is enough to use the locally constant field approximation. Then the probability of photon emission by an electron (positron) with energy  $\varepsilon$  is readily given by the formula<sup>13</sup>

$$W_{rad} = \frac{\alpha m^2 c^4}{3^{3/2} \pi \hbar \varepsilon} \int_0^\infty du \frac{5u^2 + 7u + 5}{(1+u)^3} K_{2/3} \left( \frac{2u}{3\chi} \right), \quad (2)$$

$$W_{rad} \approx 1.44 \frac{\alpha m^2 c^4}{\pi \hbar \varepsilon} \chi, \quad \chi \ll 1, \quad (3)$$

$$W_{rad} \approx 1.46 \frac{\alpha m^2 c^4}{\hbar \varepsilon} \chi^{2/3}, \quad \chi \gg 1, \quad (4)$$

where  $\alpha = e^2/\hbar c$  is the fine structure constant and  $K_\nu(x)$  is the McDonald function<sup>14</sup>. The radiation process can be treated classically in the limit  $\chi \ll 1$ . In this limit the photon emission probability is determined by Eq. (3). The quantum nature of photon emission manifests itself (for example, through the spin and the recoil effects) at high intensities or for high energy,  $\chi \geq 1$ . In the limit  $\chi \gg 1$  the probability becomes a nonlinear function of the electron energy and the electromagnetic field strength and is reduced to Eq. (4).

Pair photoproduction in a strong electromagnetic field is a cross channel of photon emission<sup>12</sup>. It's determined by similar QED parameter  $\chi_{ph}$ , which is defined by Eq. (1), where  $\varepsilon$  and  $\mathbf{p}$  are substituted by the photon energy  $\varepsilon_{ph}$  and the photon momentum  $\mathbf{p}_{ph}$ . The probability of pair production is given by the formulas (see also<sup>11</sup>)

$$W_{pair} = \frac{\alpha m^2 c^4}{3^{3/2} \pi \hbar \varepsilon_{ph}} \int_0^1 du \frac{9-u^2}{1-u^2} K_{2/3} \left( \frac{8u/3\chi_{ph}}{1-u^2} \right), \quad (5)$$

$$W_{pair} \approx 0.23 \frac{\alpha m^2 c^4}{\hbar \varepsilon_{ph}} \chi_{ph} \exp \left( -\frac{8}{3\chi_{ph}} \right), \quad \chi_{ph} \ll 1, \quad (6)$$

$$W_{pair} \approx 0.38 \frac{\alpha m^2 c^4}{\hbar \varepsilon_{ph}} \chi_{ph}^{2/3}, \quad \chi_{ph} \gg 1 \quad (7)$$

Unlike the photon emission, the pair production probability turns exponentially small in the quasiclassical limit  $\chi_{ph} \ll 1$ .

Photon emission and pair photoproduction are not efficient if the initial particle and the electromagnetic wave propagate in the same directions. QED cascading may occur in a single plane electromagnetic wave if the seed counter-propagates the wave, however it decays quickly since the produced electron-positron pairs are pushed by the field mostly along the direction of propagation of the wave. However, it was shown<sup>3,15</sup> that cascades can develop efficiently in a standing electromagnetic wave, which can be generated by two counter-propagating laser pulses. As the pair production probability vanishes exponentially as the field strength decreases, there must exist a vague threshold value of the laser intensity required for cascading. Estimations show<sup>4</sup> that cascade development becomes possible for lasers with intensities of the order of  $10^{25}$  W/cm<sup>2</sup>. Numerical simulations<sup>5</sup> had demonstrated that the actual threshold is even lower.

Cascade origination and development is a rather complex phenomenon due to interplay between the QED and plasma effects, hence in most cases numerical simulations are the only tool to explore it. A typical numerical scheme taking proper account of QED effects for modeling laser plasma dynamics combines a particle-in-cell (PIC) and Monte-Carlo (MC) methods<sup>5,16-19</sup>. The trajectories of the particles and the distribution of the laser-plasma fields are calculated by the PIC method while the photon emission and pair photoproduction is modelled with MC method. The validity of PIC and MC methods is justified because the formation lengths of the processes of emission of  $\gamma$ -quanta and pair production are much less than both the laser wavelength and the mean free path of the cascade particles<sup>20,21</sup>. The  $\gamma$ -quanta can be treated in simulation as particles while the low-frequency laser and plasma fields can be calculated by integrating Maxwell equations.

PIC-MC simulations have been used to evaluate the laser intensity threshold for cascade production<sup>20-22</sup>, as well as to study the nonlinear stage of QED cascade with strong plasma absorption of the laser field<sup>5</sup>. Up to now, the self-consistent numerical modeling of QED used to be restricted by two dimensions. Obviously, an extension to 3D would be a goal because particle motion in those field configurations which are interesting for applications is usually essentially three-dimensional. Here we report the results of 3D simulation of QED cascading in the field of long counter-propagating laser pulses. In order to study polarization effect and to exclude influence of the other laser parameters (like pulse duration and pulse radius) we consider the field configuration, which is close to the standing electromagnetic field.

The impact of polarization of the laser field on QED cascading has been studied with numerical model based on the assumption that electron radiation losses occur continuously and thus can be governed by some modified version of the Landau-Lifshitz equation<sup>15</sup>. Another drawback of such a model was that it allowed to analyse only the first generation of cascade particles. Here we employ 3D PIC-MC simulation, which is free from all such assumptions and limitations. We also extended the qualitative model of QED cascade. In the current paper, we only focus on the early stages of cascade development, when the electromagnetic self-field of the arising electron-positron plasma can still be neglected.

The paper is organized as follows. In Sec. II the results of numerical simulations by 3D PIC-MC code are presented. In order to comment on and explain them, an analytical model is developed in Sec. III. Finally, conclusion and discussion of the results are collected in Sec. IV.

## II. NUMERICAL SIMULATION

### A. Circular polarization

Consider first the QED cascading driven by circularly polarized (CP) laser pulses. We approximate the wave field by the field of two counter-propagating long laser pulses, assume that pulses counter-propagate along  $x$  axis and choose the initial condition for the laser field at  $t = 0$  in the form

$$E_y = g(y, z) [f_2(x + x_0) - f_2(x - x_0)], \quad (8)$$

$$E_z = g(y, z) [-f_1(x + x_0) - f_1(x - x_0)], \quad (9)$$

$$B_y = g(y, z) [-f_1(x - x_0) + f_1(x + x_0)], \quad (10)$$

$$B_z = g(y, z) [f_2(x + x_0) + f_2(x - x_0)], \quad (11)$$

$$g(y, z) = a_0 \cos^2\left(\frac{y}{\sigma_r}\right) \cos^2\left(\frac{z}{\sigma_r}\right) \quad (12)$$

$$f_1(x) = \cos(x) \cos^2\left(\frac{x}{\sigma_x}\right) \quad (13)$$

$$f_2(x) = \sin(x) \cos^2\left(\frac{x}{\sigma_x}\right) \quad (14)$$

where the field strengths are normalized to  $mc\omega_L/|e|$ ,  $a_0 = eE_0/mc\omega_L$ ,  $E_0$  is the electric field amplitude of a single laser pulse,  $\omega_L$  is the laser pulse cyclic frequency,  $x_0$  is a half of

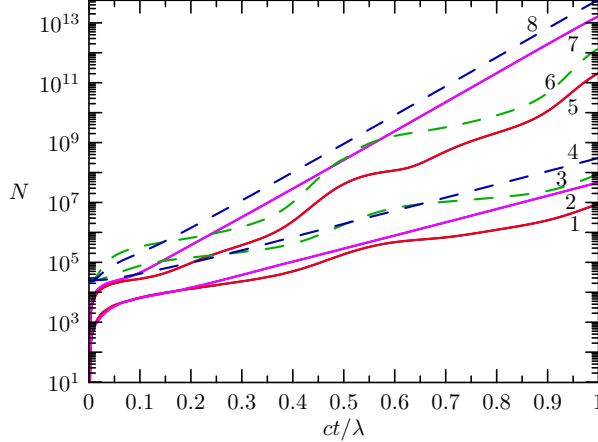


FIG. 1. Time dependence of the number of electrons (positrons) in a QED cascade in LP laser field for  $a_0 = 2.83 \times 10^3$  (red solid line 1), and  $a_0 = 8.0 \times 10^3$  (red solid line 5) and in CP laser field for  $a_0 = 2.0 \times 10^3$  (magenta solid line 2) and  $a_0 = 5.66 \times 10^3$  (red solid line 7). Time dependence of the number of  $\gamma$ -quanta in a QED cascade in LP laser field for  $a_0 = 2.83 \times 10^3$  (green dashed line 3), for  $a_0 = 8.0 \times 10^3$  (green dashed line 6) and in CP laser field for  $a_0 = 2.0 \times 10^3$  (blue dashed line 4), and  $a_0 = 5.66 \times 10^3$  (blue dashed line 8).

the initial distance between the laser pulses. The parameters of simulations are  $\sigma_x = 53\lambda$ ,  $\sigma_r = 3\lambda$ ,  $x_0 = 5\lambda$ , where  $\lambda = 2\pi c/\omega_L = 0.91\mu\text{m}$  is the laser wavelength. The cascade is initiated by a bunch of MeV-photons moving along the  $x$  axis with a center located initially at  $y = z = 0$  and  $x = -x_0$ . The length and the radius of the photon bunch are  $4\lambda$  and  $0.1\lambda$ , respectively. Cascading is explored for two values of laser intensity, corresponding to  $a_0 = 2.0 \times 10^3$  and  $a_0 = 2^{-1/2} \cdot 8000 = 5.66 \times 10^3$ .

The results of the simulation are shown in Figs. 1-6. It follows from Fig. 1 that the number of pairs is growing exponentially.  $N \propto \exp(\Gamma t)$ , up to  $4 \times 10^7$  and  $2 \times 10^{13}$  during a laser period for  $a_0 = 2.0 \times 10^3$  and  $a_0 = 5.66 \times 10^3$ . Accordingly, the cascade growth rate can be estimated as  $\Gamma \simeq 3.3\omega_L$  and  $\Gamma \simeq 7.1\omega_L$ , respectively (see Figs. 2 and 3). In particular, the inverse cascade growth rate is much shorter than the laser period. The ratio of the numbers of photons and pairs is about 3.4 for and 1.7 (see Fig. 4). As can be observed from Fig. 6, the electron-positron plasma is produced mostly near the plane  $B = 0$ . The normalized energy spectra of the electrons and positrons produced in the cascade are shown in Fig. 5 at two random successive time instances for both value of  $a_0$ , it becomes clear that the shape of the spectra remains conserved in time. The mean energy of electrons and positrons is

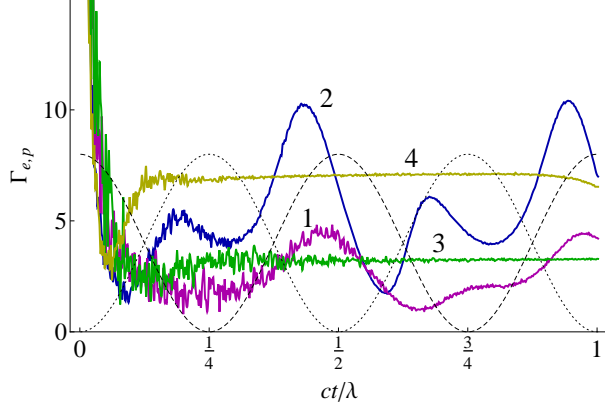


FIG. 2. Evolution of the growth rates of pairs (solid lines) in LP laser field with  $a_0 = 2.83 \times 10^3$  (line 1),  $a_0 = 8.0 \times 10^3$  (line 2) and in CP laser field with  $a_0 = 2.0 \times 10^3$  (line 3),  $a_0 = 5.66 \times 10^3$  (line 4), along with the electric field strength (in arbitrary units) at the  $B$ -node location (dotted line) and the magnetic field strength (in arbitrary units) at the  $E$ -node location (dashed line).

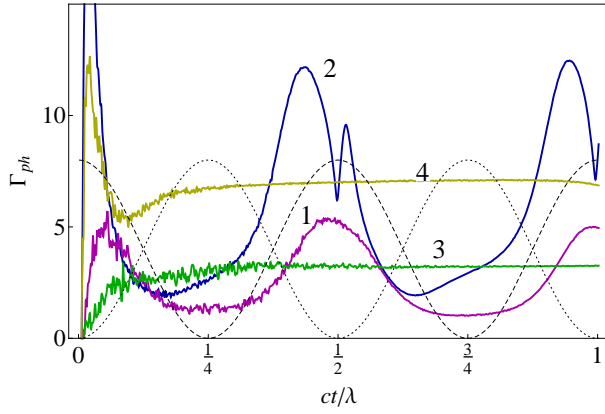


FIG. 3. The photon number growth rates (solid lines) as function of  $ct/\lambda$  in LP laser field with  $a_0 = 2.83 \times 10^3$  (line 1),  $a_0 = 8.0 \times 10^3$  (line 2) and in CP laser field with  $a_0 = 2.0 \times 10^3$  (line 3),  $a_0 = 5.66 \times 10^3$  (line 4). The electric field strength (in arbitrary units) at the  $B$ -node location (dotted line) as function of  $ct/\lambda$  and the magnetic field strength (in arbitrary units) at the  $E$ -node location (dashed line) as function of  $ct/\lambda$ .

around 500 MeV for  $a_0 = 2.0 \times 10^3$  and 1 GeV for  $a_0 = 5.66 \times 10^3$ .

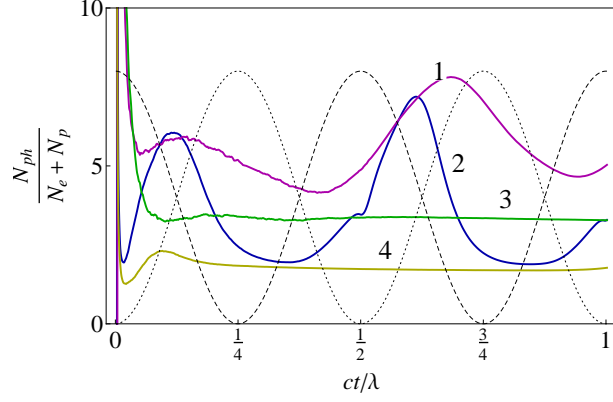


FIG. 4. Time dependence of the ratio of the numbers of photons and pairs in LP laser field with  $a_0 = 2.83 \times 10^3$  (line 1),  $a_0 = 8.0 \times 10^3$  (line 2) and in CP laser field with  $a_0 = 2.0 \times 10^3$  (line 3),  $a_0 = 5.66 \times 10^3$  (line 4), along with the electric field strength (in arbitrary units) at the  $B$ -node location (dotted line) and the magnetic field strength (in arbitrary units) at the  $E$ -node location (dashed line).

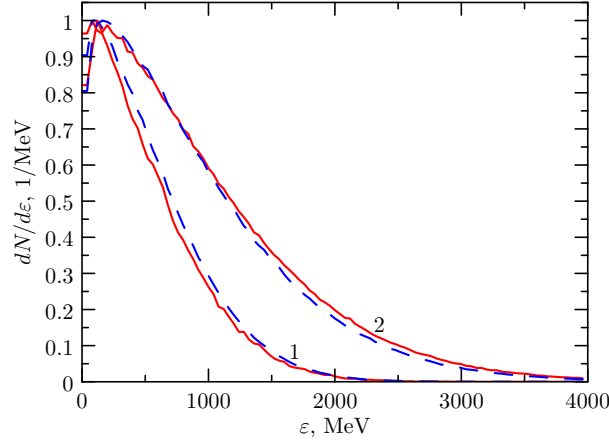
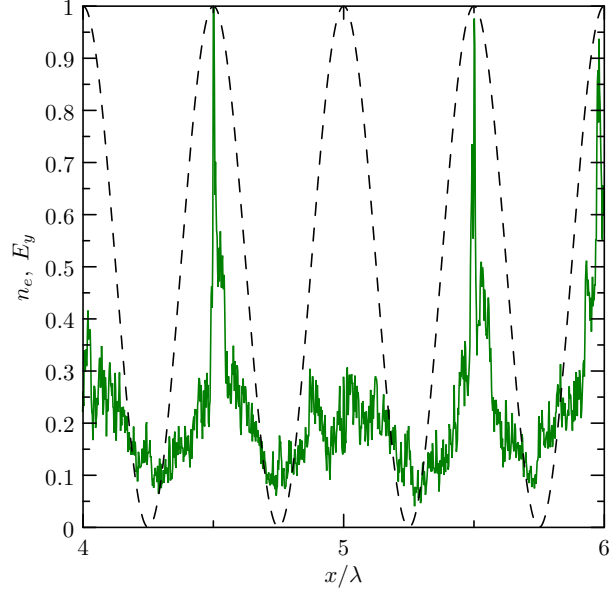
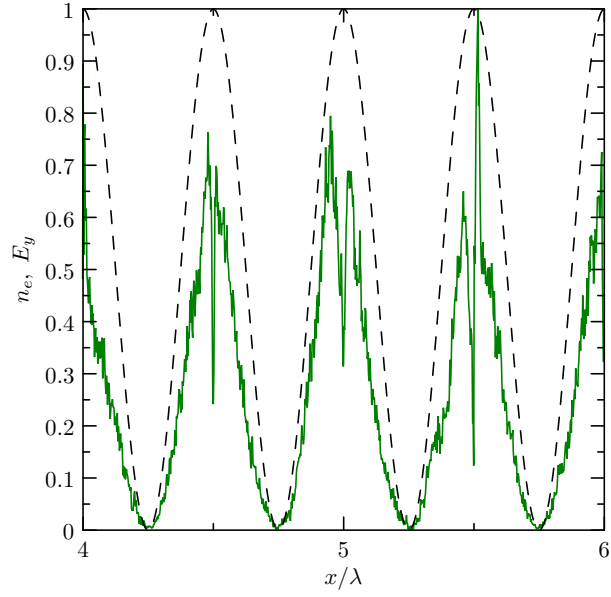


FIG. 5. The normalized energy spectra of the electron-positrons pairs produced in QED cascade in CP laser field at the instance  $t = 1.6\lambda/c$  (red solid line 1) and  $t = 2\lambda/c$  (blue dashed line 1) for  $a_0 = 2.0 \times 10^3$ ; the same at  $t = 0.6\lambda/c$  (red solid line 2) and  $t = 1.0\lambda/c$  (blue dashed line 2) for  $a_0 = 5.66 \times 10^3$ .





a)



b)

FIG. 6. Electric field strength normalized to the amplitude (black dashed line) and pair density normalized to its maximum value (green solid line) as functions of  $x$  at the instance  $t = 2\lambda/c$  in CP laser field for a)  $a_0 = 2.0 \times 10^3$ , b)  $a_0 = 2^{-1/2} \cdot 8000$ .

## B. Linear polarization

Now consider QED cascading driven by linearly polarized (LP) laser pulses. The components of the laser field at  $t = 0$  are

$$E_y = a_0 g(y, z) [f_1(x + x_0) - f_1(x - x_0)], \quad (15)$$

$$E_z = B_y = 0,$$

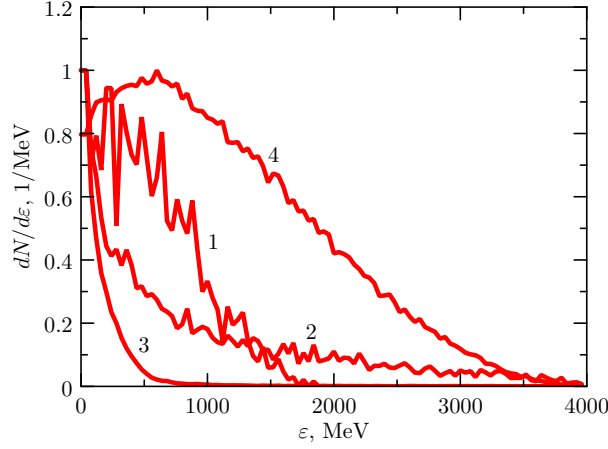
$$B_z = a_0 g(y, z) [f_1(x + x_0) + f_1(x - x_0)]. \quad (16)$$

In order to simplify the mapping with the previous CP case, we assume the same power and energy of the pulses, thus considering the value  $a_0 = 2^{1/2} \cdot 2000 = 2.83 \cdot 10^3$  and  $a_0 = 2^{1/2} \cdot 2000 = 8.0 \times 10^3$ , with all the other parameters being the same as before. As is shown in Fig. 1, the number of pairs is growing during a laser period this time up to  $10^7$  and  $2 \times 10^{11}$  for the chosen value of  $a_0$ . However, in the present case the cascade growth rate oscillates from  $\sim 0.9\omega_L$  to  $\sim 4.5\omega_L$  for  $a_0 = 2.83 \times 10^3$  and from  $\sim 1.8\omega_L$  to  $\sim 10.4\omega_L$  for  $a_0 = 8.0 \times 10^3$  (see Figs. 2 and 3). The photon-pair ratio oscillates from 4.2 to 7.8 and from 1.9 to 7.2, respectively (see Fig. 4). Hence, unlike the CP case, the number of the cascade particles is increasing in time stair-step-like at the logarithmic scale.

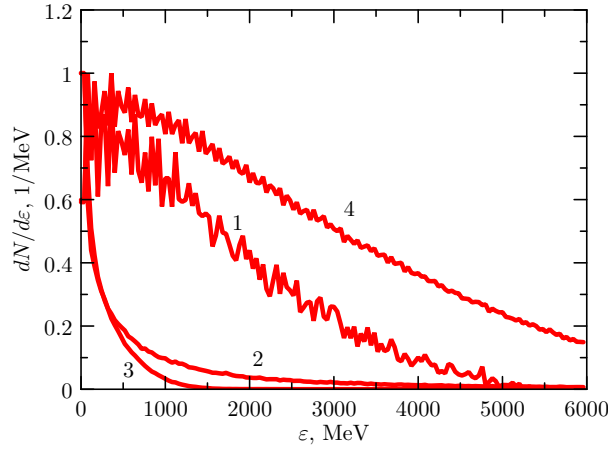
The energy spectra of the electrons and positrons produced in a QED cascade is depicted in Fig. 7 for several successive time moments. The distribution function of the cascade particles is breathing with the period, which equals to a half of the laser period. During  $0.2\lambda/c < t < 0.4\lambda/c$  a moderate growth of the number of particles accompanying by plasma heating can be observed. Note that this time interval stands out for the the volume of the spatial region where  $|\mathbf{E}(x, t)| > |\mathbf{B}(x, t)|$  (the "electric" region) is larger than of the region where  $|\mathbf{E}(x, t)| < |\mathbf{B}(x, t)|$  (the "magnetic" region) and that the electron-positron plasma is mostly located near the plane  $E = 0$  (see Fig. 8). During  $0.4\lambda/c < t < 0.55\lambda/c$  particle production peaks but the mean energy decreases. Lastly, during  $0.55\lambda/c < t < 0.7\lambda/c$  particle production becomes strongly suppressed but the mean energy per particle reaches a minimum. For this time interval the volume of the "electric" region becomes smaller than that of the "magnetic" region and the electron-positron plasma density has two maximums around each of the planes  $E = 0$  (see Fig. 9).

The mean energy per particle oscillates between a small value and 1.5 GeV for  $a_0 = 2.83 \times 10^3$  or 3 GeV for  $a_0 = 8.0 \times 10^3$ , respectively (see Fig. 7). It peaks at  $t = 0.25\lambda/c$

and  $7 = 0.75\lambda/c$  when the "electric" region occupies all space and becomes minimal at  $t = 0.5\lambda/c$  and  $t = \lambda/c$  when per contra the "magnetic" region extends to all the space.



a)



b)

FIG. 7. The normalized energy spectra of the electron-positron pairs produced in QED cascade in LP laser field for a)  $a_0 = 2.83 \times 10^3$  at the time instances  $t = 1.2\lambda/c$  (line 1),  $t = 1.4\lambda/c$  (line 2),  $t = 1.6\lambda/c$  (line 3),  $t = 1.8\lambda/c$  (line 4); b)  $a_0 = 8.0 \times 10^3$  at the time instances  $t = 0.2\lambda/c$  (line 1),  $t = 0.4\lambda/c$  (line 2),  $t = 0.6\lambda/c$  (line 3),  $t = 0.8\lambda/c$  (line 4).

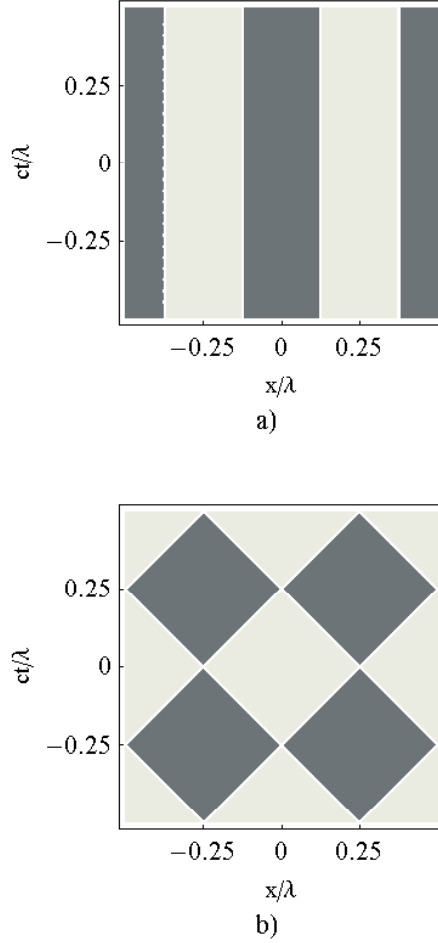
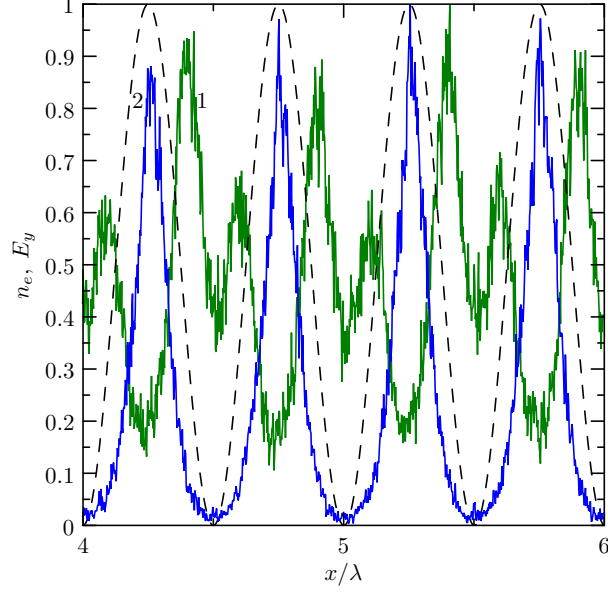


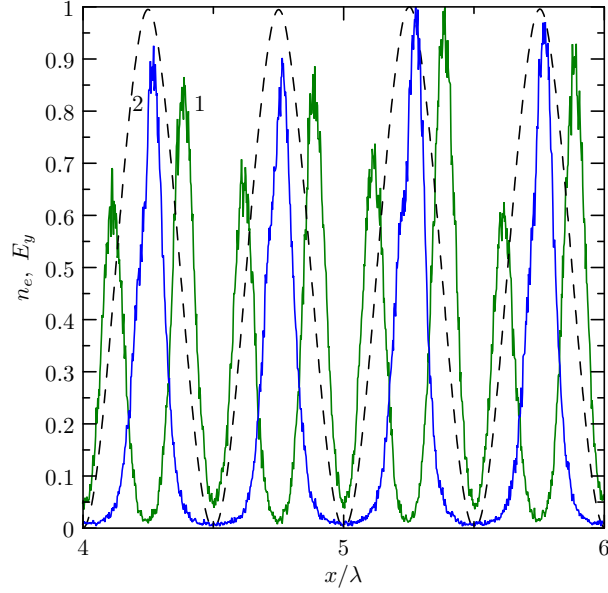
FIG. 8. The “electric” region, where the electric field is stronger than the magnetic one, (dark gray area) and “magnetic” region, where the magnetic field is stronger than the electric one, (light gray area) in  $x - t$  plane for the circularly (a) polarized standing electromagnetic wave and for the linearly polarized standing electromagnetic wave (b).

### C. Comparison of cascading in CP and LP fields

The time dependence of the number of particle in a cascade can be generally parametrized as  $N(t) \propto \exp(\int \Gamma dt)$ , where  $\Gamma$  is the instantaneous cascade growth rate. In the LP case the growth rate  $\Gamma_{LP}(t)$  is a periodical function with the period being a half of the laser period, and so on the energy spectra. Accordingly, the number of particles is growing stair-step-like at the logarithmic scale. This contrasts the CP case, in which the cascade growth rate



a)



b)

FIG. 9. The electric field strength normalized to the filed amplitude (red dashed line) and the plasma density normalized to the density maximum (green solid line) at the time instance  $t = 1\lambda/c$  in LP laser field for a)  $a_0 = 2.83 \times 10^3$ , b)  $a_0 = 8.0 \times 10^3$ .

$\Gamma_{LP}(t)$  and pair spectra remain constant while the particle number is growing exponentially.

The number of cascade particles produced at  $t = 2\lambda/c$  in LP field is on the case  $a_0 = 2.83 \times 10^3$  approximately a quarter of those in CP field with the corresponding value  $a_0 = 2.0 \times 10^3$ . As for  $a_0 = 8.0 \times 10^3$  the number of particles produced in CP field is already a

hundred times less than in LP field for  $a_0 = 5.66 \times 10^3$ . Thus, more particles are produced in CP field than in LP field for the same laser energy.

Eliminating the oscillations, the ratio of the numbers of particles for linear and circular polarisations can be cast in the form  $N_{CP}/N_{LP} \simeq \exp[(\Gamma_{CP} - \langle\Gamma_{LP}\rangle)t]$ , where  $\langle\Gamma_{LP}\rangle$  is the average over a period of the LP case growth rate. For the two sets of  $a_0$  under consideration this quantity is around  $1.4\omega_L$  and  $4.7\omega_L$ , respectively. One can also introduce a polarisation factor as the ratio of the cascade growth rates for LP and CP cases,  $\langle\Gamma_{LP}\rangle/\Gamma_{CP}$ , which acquires the value 0.85 and 0.8, respectively, i. e. has an advantage that it depends rather weakly on  $a_0$ . As for the mean energy per particle, for our parameters it's found around three times higher in LP case than in CP case. This is rather natural in a view of the previous discussion, because cascading obviously tends to suppress most of all the high energy population of plasma particles.

### III. ANALYTICAL MODEL

#### A. General consideration

In this Section we develop simple analytical model for QED cascading in the standing electromagnetic wave of arbitrary polarization so that the field components are functions of  $x$  and  $t$  only. The dynamics of the cascade particles is governed by the kinetic equations<sup>1,21</sup>. However the cascade kinetic equations cannot be solved analytically in general case. Here we will use more simple approach based on analysis of cascade particle dynamics<sup>4</sup>. For simplicity we assume that the cascade particles double within the time interval much lower than the laser period, that is  $\Gamma \gg 1$ . We also assume that  $\chi \gg 1$  for the most of electrons and positrons when they emit photons and  $\chi_{ph} \gg 1$  for the most photons when they decay with electron-positron pair production. In the limit  $\chi \gg 1$  the energy for the most of the electrons (positrons) after photon emission is much lower than that before emission.

The continuity equation for the cascade particle density can be written as follows

$$\frac{\partial n}{\partial t} + \frac{\partial}{\partial x}(v_x n) - \Gamma n = 0, \quad (17)$$

where  $n$  is the density of the cascade particles and  $v$  is the particle velocity. As  $\Gamma \gg 1$ ,  $v_x < 1$  and the particle displacement between QED events is small  $\delta x \sim 1$  the second term in Eq. (17) can be neglected. Therefore we can conclude that the most of the particles are

produced at a given space point rather than come from neighbourhood locations and we can exclude the space motion of the cascade particles from consideration. Neglecting the motion of the cascade particles, the equations for the numbers of particles take a form:

$$\frac{dN_{e+p}}{dt} = 2W_{pair}N_{\gamma}, \quad (18)$$

$$\frac{dN_{\gamma}}{dt} = W_{em}N_{e+p} - W_{pair}N_{\gamma}, \quad (19)$$

where  $N_{e+p}$  is the number of the electrons and positrons and  $N_{\gamma}$  is the number of the photons. Solving the equations we find that  $N \propto \exp \Gamma t$ , where

$$\Gamma = \frac{W_{pair}}{2} \left( -1 + \sqrt{1 + \frac{8W_{rad}}{W_{pair}}} \right), \quad (20)$$

$$\frac{N_{\gamma}}{N_{e+p}} = \frac{\Gamma}{2W_{pair}}, \quad (21)$$

where Eqs. (4) and (7) are used for  $W_{rad}$  and  $W_{pair}$ , respectively.

To estimate the cascade growth rate we should calculate temporal evolution of  $\gamma$  and  $\chi$  for the test cascade particle. The electron dynamics between the time moments of photon emission is governed by equations of motion

$$\frac{d\mathbf{p}}{dt} = -\mathbf{E} - \left[ \frac{\mathbf{p}}{\gamma} \times \mathbf{B} \right], \quad (22)$$

$$\frac{d\mathbf{r}}{dt} = \frac{\mathbf{p}}{\gamma}. \quad (23)$$

where  $\mathbf{p}$  is normalized to  $mc$ ,  $\gamma$  is gamma-factor of the particle,  $t$  is normalized to  $\omega_L^{-1}$ , the coordinates are normalized to  $c/\omega_L$ , the electromagnetic field strength is normalized to  $m c \omega_L / |e|$ . The equation for positron motion can be derived from Eqs. (22) and (23) replacing  $e$  by  $-e$ . In the laser field with normalized field strength  $a$  the gamma-factor of the particle is limited by  $a$ . As the electron lost most of its energy after photon emission we suppose that the electron is initially ( $t = t_0$ ) at rest (just after photon emission).

The characteristic times of elementary cascade processes like photon emission and pair production are much smaller than laser period  $t_{rad}, t_{pair} \ll 1$  for typical cascade conditions<sup>4,20</sup>, where  $t_{rad} \approx W_{rad}^{-1}$  and  $t_{pair} \approx W_{pair}^{-1}$  are the characteristic times of photon emission and pair production, respectively. Therefore we can solve Eqs. (22) and (23) expanding solution in Taylor series in  $\delta t \ll 1$  near  $t = t_0$ . The first-order term of  $\gamma$  can be presented as follows  $\gamma = (\delta t) a k_{\gamma}(x_0, t_0)$ , where  $k_{\gamma}(x_0, t_0)$  is a function of the electromagnetic field strength in the initial time instant and in the initial electron position  $x_0 = x(t = t_0)$ .

It follows from Eq. (1) that the parameter  $\chi$  is approximately equal to the product of  $\gamma$  and the force component which is transverse to the electron momentum. The last is vanishing at  $t = t_0$  as the electron first moves along the force direction. So,  $\chi = (\delta t)^2 a \eta k_\chi(x_0, t_0)$ , as  $\chi \propto \phi a \gamma$  and the angle between the electron velocity and Lorentz force is  $\phi \sim \delta t$  to the first order in  $\delta t$ , where  $\eta = \hbar \omega_L / (mc^2)$  and  $k_\chi(x_0, t_0)$  is again function of the field components at the initial moment of time and in the initial electron position. The  $k$ -factors for CP and LP standing wave are calculated in Appendixes.

Combining formulas for  $\gamma$ ,  $\chi$  and  $W_{rad}$  the closed system of equations for the electron (positron) can be derived

$$\gamma \approx a t_{rad} k_\gamma, \quad (24)$$

$$\chi \approx a^2 t_{rad}^2 \eta k_\chi, \quad (25)$$

$$W_{rad} \approx t_{rad}^{-1} \approx 1.4 \alpha \eta^{-1} \gamma^{-1} \chi^{2/3}. \quad (26)$$

$t_{rad}$  can be excluded from the system so that the system can be expressed through the electromagnetic field parameters

$$\chi \approx (a_* \eta k_\gamma)^{3/2}, \quad (27)$$

$$\gamma \approx a_*^{3/4} \eta^{1/4} k_\chi^{-1/2} k_\gamma^{7/4}, \quad (28)$$

$$W_{rad} \approx 1.4 \alpha a_*^{1/4} \eta^{-1/4} k_\chi^{1/2} k_\gamma^{-3/4}, \quad (29)$$

where  $a_* = a(1.4\alpha)^{-1}$ . As the photon absorbs substantial portion of the electron energy and it is emitted in the direction of the electron velocity just before emission, we can assume for the sake of simplicity  $\gamma_{ph} = \gamma \gg 1$  and  $\chi_{ph} = \chi \gg 1$  so that  $W_{rad} \approx (1.46/0.38)W_{pair}$

$$\Gamma \approx 1.22 W_{rad}, \quad (30)$$

$$\frac{N_\gamma}{N_{e+p}} \approx 2.34. \quad (31)$$

It's worth to note that this relations are universal and valid for both circular polarisation and "electric" region of linear polarisation for the high intensities. We can find the numerical confirmation of this assertion in the Fig. 4, where the line 4 (circular polarisation, high intensity) and parts of line 2 (linear polarisation, high intensities), corresponding to the electric region, is in agreement with Eq. (31). Making use of Eq. (27), we can estimate  $\chi \approx 2.14$  for  $a_0 = 2^{1/2} \cdot 2000$  and  $\chi \approx 10.18$  for  $a_0 = 8000$ , where  $k_\chi$  and  $k_\gamma$  are assumed to



be of the order of unity,  $a = 2a_0$  is taken into account for the standing wave and  $\lambda = 0.91\mu m$ . Therefore, the model better fits for numerical simulations with higher  $a_0$ .

The model presented above is not valid for QED cascading in LP standing plane wave in the “magnetic” space-time region where  $|\mathbf{B}| > |\mathbf{E}|$ . As  $\mathbf{B} \perp \mathbf{E}$  for LP plane wave we can choose the reference frame where  $\mathbf{E}' = 0$  at the given time moment at the given position. It is shown in Appendix that the electron dynamics in the “magnetic” region is close to the superposition of electron Larmor rotation and the slow drift without significant energy gain. Moreover, the photon emission leads to a rapid electron cooling there.

In the ”magnetic” frame the field can be considered as static and homogeneous as  $t_{rad} \ll 1$  and the theory developed by Akhiezer *et. al*<sup>23</sup> for QED cascading in a magnetic field can be used to analyse cascade dynamics. In this case the energy of the cascade particles is limited by the energy of the first particle which initiated the cascade. The theory predicts that the cascading and particle production occur until the time moment when the energy of the cascade particles will be so low that  $\chi$  becomes lower than 1 for all particles. The estimates for the total number of the produced particles,  $N_B$ , and the characteristic time of cascade development,  $t_B$ , can be obtained from the theory:

$$N_B = \gamma a \eta, \quad (32)$$

$$t_B = \frac{81}{32} \left[ \Gamma\left(\frac{4}{3}\right) \Gamma\left(\frac{2}{3}\right) \right]^{-1} \frac{\gamma^{1/3}}{q} \gamma_B, \quad (33)$$

$$V_b = \frac{|\mathbf{E}|}{|\mathbf{B}|}, \quad (34)$$

$$\gamma_B = \frac{|\mathbf{B}|}{\sqrt{\mathbf{B}^2 - \mathbf{E}^2}}, \quad (35)$$

where  $V_b$  and  $\gamma_B$  are the velocity and the gamma-factor determining the ”magnetic” reference frame, respectively,  $t_b$  is a characteristic cascade duration (which can be estimated as a number of events  $\log \chi_0$  times time of a one event  $1/W$ ) and  $q$  is given by

$$q = \frac{\alpha 3^{1/6}}{2\pi} \Gamma\left(\frac{2}{3}\right) \left( \frac{a^2}{\eta^2 (1 + V_B)^2 \gamma_B^2} \right)^{1/3}. \quad (36)$$

The derived equations can be applied to estimation of the cascade growth rate for linear polarization in “magnetic” region

$$\Gamma_B \approx \frac{1}{t_B} \ln N_B. \quad (37)$$

Although the particle number increase non-exponentially in the “magnetic” region we have introduced  $\Gamma$  by the same way as it had been done for the exponential growth in the “electric” region (see Eq. (20)).

## B. Circular polarization

First we analyse CP as the most simple type of polarization. The dimensionless vector-potential, electric and magnetic fields of such field configuration are given by

$$\mathbf{A} = a(0, \cos x \sin t, \cos x \cos t), \quad (38)$$

$$\mathbf{E} = a(0, \cos x \cos t, -\cos x \sin t), \quad (39)$$

$$\mathbf{B} = a(0, -\sin x \cos t, \sin x \sin t). \quad (40)$$

where fields rotate around the  $x$ -direction. The invariant  $\mathcal{F} = \mathbf{E}^2 - \mathbf{B}^2$  for LP standing wave takes a form

$$\mathcal{F} = a^2 \cos 2x. \quad (41)$$

It follows from Eq. (41) that  $\mathcal{F}$  is conserved in time for CP standing wave. As It follows from the definition of  $\mathcal{F}$  (see also Fig. 4) that  $\mathcal{F} > 0$  in the “electric” region,  $\mathcal{F} < 0$  in the “magnetic” region and  $\mathcal{F} = 0$  on the border between regions. The coefficients  $k_\chi$  and  $k_\gamma$  for CP are derived explicitly in Appendix:

$$k_\chi(x) = \sqrt{\frac{\cos^2 x}{\tan^2 x + 4}}, \quad k_\gamma = \cos x_0. \quad (42)$$

The factors are time-independent as well as  $\mathcal{F}$ . At  $x = 0$  we have  $k_\chi = 1/2$ ,  $k_\gamma = 1$ , and Eqs. (29) reduced to that derived in Ref. <sup>4</sup>. Making use of Eqs. (29) and (42) the cascade growth rate can be calculated. Analysis of the rate shows that the cascade rate is almost constant for  $-\pi/3 + \pi l < x < \pi/3 + \pi l$ ,  $l \in Z$ . This is close to what follows from plasma distribution obtained in numerical simulation for high-intensity example (see Fig. 6 b)).

The model ratio of the photon number to the pair number is given by Eq. (27) and is close to the value obtained from numerical simulation for  $a_0 = 2^{-1/2} \cdot 8000$  (see Fig. 4). The model predicts that  $\Gamma \approx 5.6$ ,  $\epsilon \approx 400$  MeV for  $a_0 = 2000$  and  $\Gamma \approx 6.8$  for  $a_0 = 2^{-1/2} \cdot 8000$ ,  $\epsilon \approx 800$  MeV. As expected the prediction for  $a_0 = 2^{-1/2} \cdot 8000$  is in better agreement with numerical results demonstrated in Figs. 5 and Figs. 2 than that for the low-intensity case.

### C. Linear polarization

Now we analyse QED cascading in LP standing wave. The dimensionless vector-potential, electric and magnetic fields are

$$\mathbf{A} = a(0, -\cos x \sin t, 0) \quad (43)$$

$$\mathbf{E} = a(0, \cos x \cos t, 0), \quad (44)$$

$$\mathbf{B} = a(0, 0, \sin x \sin t). \quad (45)$$

Please note that the phase of the laser field given by Eqs. (15) and (16) is shifted by  $\pi/2$  from the phase of the electromagnetic wave given by Eqs. (43)-(45.) The normalized QED parameter  $\mathcal{F}$  for LP standing wave takes a form

$$\mathcal{F}(x, t) = \cos 2t + \cos 2x, \quad (46)$$

where the parameter is normalized to  $a^2/2$ . It follows from Eq. (46) that  $\mathcal{F}$  is a periodic function of time with the half of the laser period and the volume of the “electric” and “magnetic” regions evolves in time (see Fig. 8). The “electric” region occupies all space twice per laser period at  $t = \pi l$ ,  $l \in Z$ , while the “magnetic” region expands up to all space at  $t = \pi/2 + \pi l$ ,  $l \in Z$ . Some electrons and positrons produced in the cascade can be first accelerated in the electric region and then radiate their energy in the magnetic region. Even immobile particle can be in the “electric” region at some time moments and in the “magnetic” region at the other time moments because the boundary between “electric” and “magnetic” regions oscillates. Therefore, the cascade dynamics in LP field is more complex than that in CP field.

In the “electric” region we can use Eq. (29), where coefficients  $k_\chi$  and  $k_\gamma$  are calculated in Appendix:

$$k_\chi^2(x, t) = \frac{\mathcal{F}(x, t) \tan^2 x (\cos^2 x + \sin^2 t)^2}{8 \cos^2 x \cos^2 t}, \quad (47)$$

$$k_\gamma^2(x, t) = \mathcal{F}(x, t). \quad (48)$$

As the coefficients depend on time, the cascade growth rate is also a function of time which agrees with Fig. (30). In general the contribution to the cascade growth rate is given by both “electric” and “magnetic” regions simultaneously. To compare our model with numerical results we consider time moments  $t = \pi l$ ,  $l \in Z$ , when the “electric” region occupies all

space. We introduce the cascade growth rate averaged over  $x$  in the “electric” region as follows

$$N(t) = N(t_0) \exp \left( \int_{t_0}^t \bar{\Gamma}_E(t') dt' \right), \quad (49)$$

$$\bar{\Gamma}_E(t) = \frac{\int n(x, t) \Gamma(t, x) dx}{\int n(x, t) dx} \quad (50)$$

where by the definition

$$n(x, t) = n(x, t_0) \exp \left( \int_{t_0}^t \Gamma(t', x) dt' \right). \quad (51)$$

Making use of the electron distribution shown in Fig.9 and Eqs.(30), (47), (48) we can estimate  $\bar{\Gamma}_E \approx 1.95$  for  $a_0 = 2^{1/2} \cdot 2000$  and  $\bar{\Gamma}_E \approx 2.53$  for  $a_0 = 8000$ , which is in a fairly good agreement with numerical results for  $ct = 0.25\lambda$  and  $ct = 0.75\lambda$ , respectively (see Fig. 2). The particle density peaks near  $x = 0$  for the time moments  $t = \pi l$ ,  $l \in Z$ . However  $\chi \approx 0$  at  $x = 0$  as follows from Eqs. (47), (25), because the charged particle moves strictly along the electric field<sup>24</sup> as always  $B = 0$  at  $x = 0$ . The particles are produced around point  $x = 0$  in the region where  $\chi > 1$  and reaches  $x = 0$  because this point is attractive for the electrons and positrons during half of the laser period. At the position where  $\chi \approx 1$  near  $x = 0$  we can estimate  $k_\chi \approx 1$  and  $k_\gamma \approx 2$  so that the mean particle energy is  $\epsilon \approx 1500$  MeV for  $a_0 = 2^{1/2} \cdot 2000$  and  $\epsilon \approx 3000$  MeV for  $a_0 = 8000$  that is in a good agreement with the numerical results (see Fig. 7).

Now let us analyse cascading in the “magnetic” region with  $|\mathbf{B}| > |\mathbf{E}|$ . It is shown in Appendix that the particle acceleration is suppressed in this region and the electrons and positrons lose almost all their energy because of photon emission. Cascading and particle production occur until the energies of the cascade particles is so low that  $\chi < 1$  for all particles. Let us assume that the electron gains the energy in the “electric” region. Then the boundary between “electric” and “magnetic” regions is shifted so that the electron finds oneself in the “magnetic” region. We can estimate the growth rate of the cascade initiated by the electron using Eqs.(32), (33). The result is  $\Gamma_B \approx 5.6$  for  $a_0 = 2^{1/2} \cdot 2000$  and  $\Gamma_B \approx 14.5$  for  $a_0 = 8000$ . We can conclude that the particle production is more efficient in the “magnetic” regions than in the “electric” ones, which is in qualitative agreement with the numerical results (see Fig. 2) demonstrating the enhanced particle production when the “magnetic” region dominates.

There are two reasons why particles are produced more efficiently in the “magnetic” region. Firstly, In the “electric” region electrons and positrons are accelerated by the laser field so the angle between the particle momentum and the Lorentz force is small. In the “magnetic” region the particles are not accelerated and the angle can be large thereby increasing  $\chi$  and enhancing the probability of the particle production. Secondly, the particle energy decreases in time in the “magnetic” region because of photon emission. This also enhances the particle production probability as the probability increases with decreasing of the particle energy (see Eqs. (4) and (7)).

The quantitative comparison of the cascade growth rate predicted by the model with that obtained numerically is difficult because cascades develops in both “electric” and magnetic” regions permanently (see Fig. 8). The “magnetic” region occupies all space at the time moments  $t = \pi/2 + \pi l, l \in Z$ . However the electrons and positrons are strongly cooled by these time moments so that the cascading is suppressed and  $\Gamma \simeq 1$ . Therefore the self-consistent theory including QED cascading instantaneously in both “electric” and “magnetic” regions is needed.

#### IV. CONCLUSIONS

In Conclusion we study QED cascading in the field of two counter-propagating laser pulses for both circular and linear polarizations. We restricted ourself by initial stages of the cascade when the particle number is small so that the self-generated plasma fields do not affect cascade dynamics. First the cascade dynamics is explored by numerical simulation with 3D PIC-MC code. The particle number increase mostly exponentially in time. The cascade growth rate, the particle spectra and the distribution of the produced plasma tend to be constant in time for CP laser field while they periodically evolve with half of the laser period for LP laser field. It is shown that for a given laser energy the number of the particles produced in the cascade with the CP laser field is greater than in the LP one.

We develop simple analytical model of QED cascading in the standing plane electromagnetic wave. The model is based on the analysis of the single particle dynamics. For simplicity we consider the limit  $\Gamma \gg 1$ . In this limit most of the particles are produced at a given space point rather than come from neighbourhood locations and we can exclude the space motion of the cascade particles from consideration. However even for low intensity case  $a_0 < 3000$

when the parameter  $\chi$  is of the order of the unity the model is in a qualitative agreement with the numerical results.

The model can explain some key features of the cascade. The cascade dynamics is governed by relativistic invariant  $\mathcal{F}$ . In the CP standing wave  $\mathcal{F}$  is constant in time, and the particle spectra and cascade growth rate become being stationary. In contrast, in the LP standing wave  $\mathcal{F}$  oscillates in time with half of the laser period, which leads to the stair-step-like dependence of the particle number on time and periodical evolution of the particle spectra. For LP laser field the cascade dynamics in the "electric" region (where electric field is stronger than magnetic one) is strongly dissimilar from that in the "magnetic" region (where the magnetic field is stronger than electric one). In the "electric" region the electrons and positrons can be accelerated by the laser field up to very high energy. Unlike that the lepton acceleration is suppressed in the "magnetic" region. Moreover, the high-energy leptons are cooled by photon emission. The spectrum evolution predicted by the model is in good agreement with the results of numerical simulation. As the volume of the "electric" and "magnetic" regions evolves periodically in time the cascade growth rate for LP laser field is also a periodic function of time with the period equal to the half of the laser period.

The model estimation of the cascade growth rate for circular polarization is in a good agreement with the numerical result even for low-intensity example when the model assumption  $\chi \gg 1$  is not strictly fulfilled. The quantitative comparison of the cascade growth rate predicted by the model for linear polarization with that obtained numerically is difficult because the cascading occurs simultaneously in both "electric" and "magnetic" regions most of time while  $\Gamma$  can be calculated only if cascade develops only in one of two regions. The self-consistent theory for linear polarization including QED cascading instantaneously in both "electric" and "magnetic" regions is needed. To explain the dynamics of the self-generated plasma distribution the self-consistent theory should also include the temporal dynamics of the plasma density and should be extended to the particles with  $\chi < 1$  as the number of such particles is large especially in the low-intensity example.

## ACKNOWLEDGMENTS

This work was partially supported in part by the Government of the Russian Federation (Project No. 14.B25.31.0008), by the Russian Foundation for Basic Research (Grants No 13-

02-00886, 13-02-00372), by Russian Federation President's grant (Grant No -5853.2013.2), by the Federal Targeted Programme Scientific and Scientific-Pedagogical Personnel of the Innovative Russia in 2009-2013 (Governmental Contract No. 14.A18.21.0773), and by the President Grants for Government Support of the Leading Scientific Schools of the Russian Federation (grant No. NSh-5992.2012.2).

## Appendix A: Electron dynamics in CP standing wave

Let's introduce normalized parameter  $\chi_0^2$ :

$$\chi_0^2 = a^{-2}\eta^{-2}\chi^2, \quad (\text{A1})$$

where  $\chi$  is given by Eq. (1),  $\mathbf{p}$  is the momentum normalized to  $mc$  and the field strength is normalized to  $a\omega_L mc/e$ . In the CP case electric and magnetic fields are parallel to each other:  $\mathbf{B} = s\mathbf{E}$ , where  $s = -\tan x_0$ . Taking into account that, we derive for  $\chi_0^2$

$$\chi_0^2 = (s^2 + 1) [(p_z E_y - p_y E_z)^2 + p_x^2 \mathbf{E}^2] + \mathbf{E}^2. \quad (\text{A2})$$

The last term can be neglected as the electron is accelerated to the relativistic energy within very short time period  $t_{rel} \sim a^{-1} \ll t_{rad}, t_{pair} \ll 1..$

We suppose that the electron was at rest at  $x = x_0$  and  $t = t_0$ . We choose axis  $y$  along  $\mathbf{E}_0 = \mathbf{E}(x = x_0, t = t_0) = s\mathbf{B}(x = x_0, t = t_0)$ , so that  $E_z = B_z = 0$  at  $x = x_0$  and  $t = t_0$ . We can expand the fields near  $x = x_0$  and  $t = t_0$

$$E_y \approx E_0 + (\partial_t E_y) \delta t + (\partial_x E_y) \delta x, \quad (\text{A3})$$

$$E_z \approx (\partial_t E_z) \delta t + (\partial_x E_z) \delta x, \quad (\text{A4})$$

where  $\delta t \ll 1$  and  $\delta x \ll 1$ . We can also expand the electron momentum components:

$$p_x \approx \frac{1}{2} p_x'' \delta t^2, \quad (\text{A5})$$

$$p_y \approx \gamma \approx p_y' \delta t, \quad (\text{A6})$$

$$p_z \approx \frac{1}{2} p_z'' \delta t^2, \quad (\text{A7})$$

where it is taken into account that the electron first moves along  $y$ -axis so that  $p_x, p_z \ll p_y$  and  $p_x' \approx p_z' \approx 0$ .

Making use of equation of motion - Eq. (22) we can derive

$$p_x'' \delta t \approx \frac{(p_y' \delta t) (s \delta t \partial_t E_z) - (\frac{1}{2} p_z'' \delta t^2) s E_0}{p_y' \delta t}, \quad (\text{A8})$$

$$p_y \approx \gamma \approx E_0 \delta t, \quad (\text{A9})$$

$$p_z'' \delta t \approx (\partial_t E_z) \delta t + \frac{(\frac{1}{2} p_x'' \delta t^2) s E_0}{p_y' \delta t}, \quad (\text{A10})$$

where  $\mathbf{B} = s\mathbf{E}$  is used and the terms, which are proportional to  $\delta x$ , are neglected as  $v_x = p_x/\gamma \ll 1$  and  $\delta x \ll \delta t$ . The solution of Eqs. (A11)-(A13) is

$$p_x \approx \frac{s}{4 + s^2} (\partial_t E_z) \delta t^2, \quad (\text{A11})$$

$$p_y \approx \gamma \approx E_0 \delta t, \quad (\text{A12})$$

$$p_z \approx \frac{2(2 + s^2)}{4 + s^2} (\partial_t E_z) \delta t^2. \quad (\text{A13})$$

Combining Eq. (A2), Eqs. (C1), (C2) and Eqs. (A11)-(A13)  $\chi_0^2$  can be derived

$$\chi_0^2 \approx (s^2 + 1) \delta t^4 \left[ d_1^2 + \frac{1}{4} (p_x'')^2 E_0 \right] \quad (\text{A14})$$

$$d_1 = \frac{1}{2} p_z'' E_0 - p_y' (\partial_t E_z) \quad (\text{A15})$$

Finally we get

$$\chi^2 = 2a^4 \eta^2 \delta t^4 k_\chi^2, \quad (\text{A16})$$

$$k_\chi^2 = \frac{\cos^2 x_0}{\tan^2 x_0 + 4}, \quad (\text{A17})$$

where Eqs. (A11)-(A13) for CP field distribution is used. The equation for gamma-factor of the electron can be written as follows

$$\frac{d\gamma}{dt} = a (\mathbf{p} \cdot \mathbf{E}). \quad (\text{A18})$$

Finally the gamma-factor is

$$\gamma = a k_\gamma \delta t, \quad k_\gamma^2 = \cos^2 x_0. \quad (\text{A19})$$

## Appendix B: Electron dynamics in LP standing wave in the “electric” region ( $|\mathbf{E}| > |\mathbf{B}|$ )

First we consider the space-time region where  $|\mathbf{E}| > |\mathbf{B}|$ . It is convenient to treat the problem in another reference frame, namely in the “electric” frame where at  $t = t_0$   $\mathbf{B}'(x'_0, t'_0) = 0$



(accent marks quantities in the “electric” reference frame). The appropriate boost’s velocity is given by

$$V_E = \frac{B_z(x_0, t_0)}{E_y(x_0, t_0)}, \quad (\text{B1})$$

where  $B_z(x_0, t_0)$  and  $E_y(x_0, t_0)$  are the electric and magnetic fields in the laboratory reference. Nearby  $(x'_0, t'_0)$  the field component can be expanded up to the first order:

$$E'_y \approx E'_0 + (\partial_{t'} E'_y) \delta t' + (\partial_{x'} E'_y) \delta x', \quad (\text{B2})$$

$$B'_y \approx (\partial_{t'} B'_z) \delta t' + (\partial_{x'} B'_z) \delta x', \quad (\text{B3})$$

It should be noted that for the field derivatives we can write

$$(\partial_{t'} E'_y) = -(\partial_{x'} B'_z), \quad (\text{B4})$$

$$(\partial_{x'} E'_y) = -(\partial_{t'} B'_z)', \quad (\text{B5})$$

Equation of the electron motion (22) can be solved with expansion in time series  $a^{-1} \ll \delta t' \ll 1$ :

$$p'_y \approx -E'_0 \delta t' - \frac{(\delta t')^2}{2} (\partial_{t'} E'_y), \quad (\text{B6})$$

$$p'_x \approx \frac{(\delta t')^2}{2} (\partial_{x'} E'_y), \quad (\text{B7})$$

where the terms of the zeroth order on  $1/a$  are kept and the terms, which are proportional to  $\delta x$  are neglected because  $\delta x \sim a^{-1} \ll \delta t'$ . The leading term for  $\chi$  takes a form

$$\chi = \frac{1}{2} E'_0 (\partial_{t'} B'_z) (\delta t')^2. \quad (\text{B8})$$

$\chi$  is the relativistic invariant. Expressing it in terms of the laboratory-frame quantities and substituting the field component for LP standing wave from Eqs. (50), (45) we obtain

$$\chi \approx \delta t^2 a^2 k_\chi, \quad (\text{B9})$$

$$k_\chi^2 = \frac{\mathcal{F}(x_0, t_0) \tan^2 x_0 (\cos^2 x_0 + \sin^2 t_0)^2}{8 \cos^2 x_0 \cos^2 t_0}, \quad (\text{B10})$$

where  $\mathcal{F}(x_0, t_0)$  is the normalized QED parameter defined by Eq. (51). It follows from Eqs. (A11) that  $\gamma' \approx |p'_y| \approx E'_0 \delta t'$ . Expressing it in terms of the laboratory-frame quantities and substituting the field component for LP standing wave we obtain

$$\gamma \approx a k_\gamma \delta t, \quad (\text{B11})$$

$$k_\gamma = \mathcal{F}(x_0, t_0). \quad (\text{B12})$$

## Appendix C: Electron dynamics in LP standing wave in the “magnetic” region ( $|\mathbf{B}| > |\mathbf{E}|$ )

Let us now consider the space-time region where  $|\mathbf{B}| > |\mathbf{E}|$ . It is again convenient to treat the problem in another reference frame, namely in the “magnetic” frame where at  $t = t_0$   $\mathbf{E}'(x'_0, t'_0) = 0$  (accent marks quantities in the “magnetic” reference frame). The appropriate boost velocity and the boost gamma-factor are given by

$$V_B = \frac{E_y(x_0, t_0)}{B_z(x_0, t_0)}, \quad (\text{C1})$$

$$\gamma_B = \frac{B_z(x_0, t_0)}{\sqrt{B_z^2(x_0, t_0) - E_y^2(x_0, t_0)}}. \quad (\text{C2})$$

where  $B_z(x_0, t_0)$  and  $E_y(x_0, t_0)$  are the electric and magnetic fields in the laboratory reference. For simplicity we will consider region, where  $B_y > 2^{1/2}E_z$  so that  $\gamma_B \sim 1$  and  $V_B\gamma_B < 1$ . Nearby  $(x'_0, t'_0)$  the field component can be expanded up to the first order:

$$E'_y \approx (\partial_{t'} E'_y) \delta t' + (\partial_{x'} E'_y) \delta x', \quad (\text{C3})$$

$$B'_z \approx B'_0 + (\partial_{t'} B'_z) \delta t' + (\partial_{x'} B'_z) \delta x', \quad (\text{C4})$$

The field derivatives obey Eqs. (B4), (B5). We suppose that in the laboratory reference frame the electron is at rest at the initial moment of time  $t = t_0$  so that in the magnetic frame  $\gamma'_0 = \gamma_B$ ,  $p'_{x,0} = -v_B\gamma_B$ ,  $p'_{z,0} = p'_{y,0} = 0$ . Assuming again that  $\delta t' \ll 1$  and keeping the leading terms, the equation of the electron motion (22) can be rewritten in the non-relativistic limit as follows

$$(\partial_{t'} p'_x) = -B'_0 p'_z, \quad (\text{C5})$$

$$(\partial_{t'} p'_y) = -t' (\partial_{t'} E'_y) - B'_0 p'_x. \quad (\text{C6})$$

The derived equations describe Larmor rotation of the electron in the magnetic field with growing electric field. The solution takes a form:

$$p'_x = p'_{x,0} \cos(B'_0 \delta t') - \delta t' \frac{(\partial_{t'} E'_y)}{B'_0}, \quad (\text{C7})$$

$$p'_y = -p'_{x,0} \sin(B'_0 \delta t') + \frac{(\partial_{t'} E'_y)}{(B'_0)^2}. \quad (\text{C8})$$

The terms proportional to  $\delta x'$  in the field expansion are neglected Eqs. (C5), (C6) because it follows from Eqs. (C7), (C8) that  $\delta x' \sim p'_{x,0}/a + (\delta t')^2/2 \ll \delta t'$ , where estimation  $B'_0 \sim (\partial_{t'} E'_y) \sim a$  is used.

Making use of Eqs. (C7), (C8) and the inverse Lorentz transformation the electron energy gain can be derived in the laboratory frame

$$\gamma = \gamma_B \sqrt{\gamma_B^2 + 2d_2 d_3 + d_3^2} - p_B(d_2 - d_3), \quad (\text{C9})$$

$$d_2 = p_B \cos(B'_0 \delta t'), \quad (\text{C10})$$

$$d_3 = \delta t' \frac{\partial_{t'} E'_y}{B'_0}. \quad (\text{C11})$$

Expressing it in terms of the laboratory-frame quantities and substituting the field component for LP standing wave, we obtain

$$\gamma = \gamma_B \sqrt{\gamma_B^2 + 2k_B p_B \delta t \cos(\omega_B \delta t) + \delta t^2 k_B^2} \quad (\text{C12})$$

$$- p_B^2 \cos(\omega_B \delta t) + k_B p_B \delta t, \quad (\text{C13})$$

$$\gamma_B = \frac{2^{1/2} \sin x_0 \sin t_0}{\sqrt{-\mathcal{F}(x_0, t_0)}}, \quad (\text{C14})$$

$$p_B = \frac{2^{1/2} \cos x_0 \cos t_0}{\sqrt{-\mathcal{F}(x_0, t_0)}}, \quad (\text{C15})$$

$$\omega_B = \frac{B_0}{\gamma_B^2} = a \frac{-\mathcal{F}(x_0, t_0)}{2 \sin x_0 \sin t_0}, \quad (\text{C16})$$

$$k_B = \frac{\partial_{t'} E'_y}{\gamma_B B'_0} = \frac{\sin 2x_0}{-\mathcal{F}(x_0, t_0)}. \quad (\text{C17})$$

where  $B_0 = B_z(x_0, t_0)$ . It follows from Eq. (C13) that  $\gamma \sim 1$  and thus there is no significant electron acceleration in contrast to the “electric” region where  $\gamma \sim a \delta t \gg 1$  (see Eq. (B11)).

## REFERENCES

- <sup>1</sup>B. Rossi, *High-Energy Particles* (Prentice-Hall, New York, 1952).
- <sup>2</sup>J. K. Daugherty, A. K. Harding, *Astrophysical Journal*, **252**, 337 (1982).
- <sup>3</sup>A. R. Bell and J. G. Kirk, *Phys. Rev. Lett.* **101**, 200403 (2008).
- <sup>4</sup>A. M. Fedotov, N. B. Narozhny, G. Mourou, G. Korn, *Phys. Rev. Lett.* **105**, 080402 (2010).
- <sup>5</sup>E. N. Nerush, I. Yu. Kostyukov, A. M. Fedotov, N. B. Narozhny, N. V. Elkina, and H. Ruhl, *Phys. Rev. Lett.* **106**, 035001 (2011).
- <sup>6</sup><http://www.extreme-light-infrastructure.eu>.

- <sup>7</sup><http://www.xcels.iapras.ru>.
- <sup>8</sup>F. Sauter, *Z. Phys.* **69**, 742 (1931).
- <sup>9</sup>N. B. Narozhny, S. S. Bulanov, V. D. Mur and V.S. Popov, *Phys. Lett. A* **330**, 1 (2004).
- <sup>10</sup>S. S. Bulanov, N. B. Narozhny, V. D. Mur and V.S. Popov, *JETP* **102**, 9 (2006).
- <sup>11</sup>A. I. Nikishov and V. I. Ritus *Proc. FIAN* **111**, 3 (1979).
- <sup>12</sup>V. B. Berestetskii, E. M. Lifshits, and L. P. Pitaevskii, *Quantum Electrodynamics* (Pergamon Press, New York, 1982).
- <sup>13</sup>V. N. Baier, V. M. Katkov and V. S. Fadin, *Radiation of the Relativistic Electrons* (Moscow: Atomizdat, 1973).
- <sup>14</sup>*Handbook of Mathematical Functions*, edited by M. Abramowitz and I. A. Stegun (Dover, New York, 1972).
- <sup>15</sup>J. G. Kirk, A. R. Bell and I. Arka, *Plasma Phys. Control. Fusion* **51**, 085008 (2009).
- <sup>16</sup>A. N. Timokhin, *Mon. Not. R. Astron. Soc.* **408**, 2092 (2010).
- <sup>17</sup>I. V. Sokolov, N. M. Naumova, J. A. Nees, G. A. Mourou, *Phys. Rev. Lett.* **105**, 195005 (2010).
- <sup>18</sup>C. P. Ridgers, C. S. Brady, R. Duclous, J. G. Kirk, K. Bennett, T. D. Arber, A. P. L. Robinson, and A. R. Bell, *Phys. Rev. Lett.* **108**, 165006 (2012).
- <sup>19</sup>E. N. Nerush, I. Yu. Kostyukov, *Nuclear Instruments and Methods in Physics Research A* **653**, 7 (2011).
- <sup>20</sup>N. V. Elkina, A. M. Fedotov, I. Yu. Kostyukov, M. V. Legkov, N. B. Narozhny, E. N. Nerush, and H. Ruhl, *Phys. Rev. ST Accel. Beams* **14**, 054401 (2011).
- <sup>21</sup>E. N. Nerush, V. F. Bashmakov, and I. Yu. Kostyukov, *Phys. Plasmas* **18**, 083107 (2011).
- <sup>22</sup>R. Duclous, J. G. Kirk and A. R. Bell, *Plasma Phys. Control. Fusion* **53**, 015009 (2011).
- <sup>23</sup>A. I. Akhiezer, N. P. Merenkov and A. P. Rekalov, *J. Phys. G: Nucl. Part. Phys.* **20**, 1499-1514 (1994).
- <sup>24</sup>S. S. Bulanov, T. Zh. Esirkepov, A. G. R. Thomas, J. K. Koga, S. V. Bulanov, *Phys. Rev. Lett.* **105**, 220407 (2010).